C.M. Juran, M.F. Dolwick, and P.S. McFetridge*

J. Crayton Pruitt Family Department of Biomedical Engineering, University of Florida, JG-56, Biomedical Sciences Building, Gainesville, FL 32611-6131, USA; *corresponding author, pmcfetridge@bme.ufl.edu

Shear Mechanics of the TMJ Disc: Relationship to Common Clinical Observations

ABSTRACT

The temporomandibular joint (TMJ) is a complex hinge and gliding joint that induces significant shear loads onto the fibrocartilage TMJ disc during jaw motion. The purpose of this study was to assess regional variation in the disc's shear loading characteristics under physiologically relevant loads and to associate those mechanical findings with common clinical observations of disc fatigue and damage. Porcine TMJ discs were compressed between an axially translating bottom platen and a 2.5-cm-diameter indenter within a hydrated testing chamber. Discs were cyclically sheared at 0.5, 1, or 5 Hz to 1, 3, or 5% shear strain. Within the anterior and intermediate regions of the disc when sheared in the anteroposterior direction, both shear and compressive moduli experienced a significant decrease from instantaneous to steady state, while the posterior region's compressive modulus decreased approximately 5%, and no significant loss of shear modulus was noted. All regions retained their shear modulus within 0.5% of instantaneous values when shear was applied in the mediolateral direction. The results of the disc's regional shear mechanics suggest an observable and predictable link with the common clinical observation that the posterior region of the disc is most often the zone in which fatigue occurs, which may lead to disc damage and perforation.

KEY WORDS: tissue engineering, temporomandibular disc, joint disease, jaw biomechanics, extracellular matrix (ECM), biomechanics.

INTRODUCTION

The temporomandibular joint (TMJ) regulates movements of the mandible with respect to the temporal bone of the skull. The fibrocartilagenous TMJ disc has, in the past decade, been the subject of more extensive mechanical evaluations. The majority of published biomechanical analyses have focused on the TMJ disc's compressive properties (Tanaka *et al.*, 2003a,e; Allen and Athanasiou, 2005; Lumpkins and McFetridge, 2009) and have found that the disc possesses significant regional variations (Lumpkins and McFetridge, 2009; Kuo *et al.*, 2010). While compressive properties are important during joint loading, the TMJ has primarily a gliding joint function that induces compressive as well as significant shear forces. Previous studies have evaluated shear under static shear loading conditions and have shown regional variations of the TMJ disc properties (Lai *et al.*, 1998). Current investigations of the TMJ under dynamic shear conditions have focused on the central region of the disc's intermediate zone (Tanaka *et al.*, 2003b, 2004; Koolstra *et al.*, 2007). The relationship between repetitive shear and compressive loading of the intervertebral disc and disc damage has been alluded to by Callaghan and Iatridis and colleagues, who suggested that disc herniation and damage may be more linked to repeated flexion extension and shear motions than to applied joint compression (Callaghan and McGill, 2001; Iatridis and ap Gwynn, 2004).

In these investigations, the regional shear and compressive characteristics of the porcine TMJ disc and the interconnectivity and dependency of these characteristics on one another and variables relevant to physiologic function have been evaluated. We hypothesized that not only is the shear modulus (G) of the TMJ disc dependent on frequency, shear, and compressive strain, but also that the compressive modulus of elasticity (E) is dependent on the application of cyclic shear loads (Lumpkins *et al.*, 2008). Additionally, we hypothesized that the interdependence of the compressive and shear elastic moduli will reveal material trends consistent with damage seen clinically in patients with temporomandibular disorders.

MATERIALS & METHODS

Specimen Preparation

Partially dissected fresh porcine TMJs were isolated from male animals ages 6 to 9 mos, purchased with IACUC approval (IACUC Protocol # 201207534) from Animal Technologies Inc. (Tyler, TX, USA). Dissection was conducted as previously described (Lumpkins *et al.*, 2008; Appendix 1). After dissection, discs were stored in 0.15 M phosphate-buffered saline (PBS, pH 7.4) at 4°C until use. All samples were stored for fewer than 12 hrs before being tested (Lumpkins *et al.*, 2008). Immediately before mechanical testing, a circular stainless steel punch with a 6-mm inner diameter was used to extract
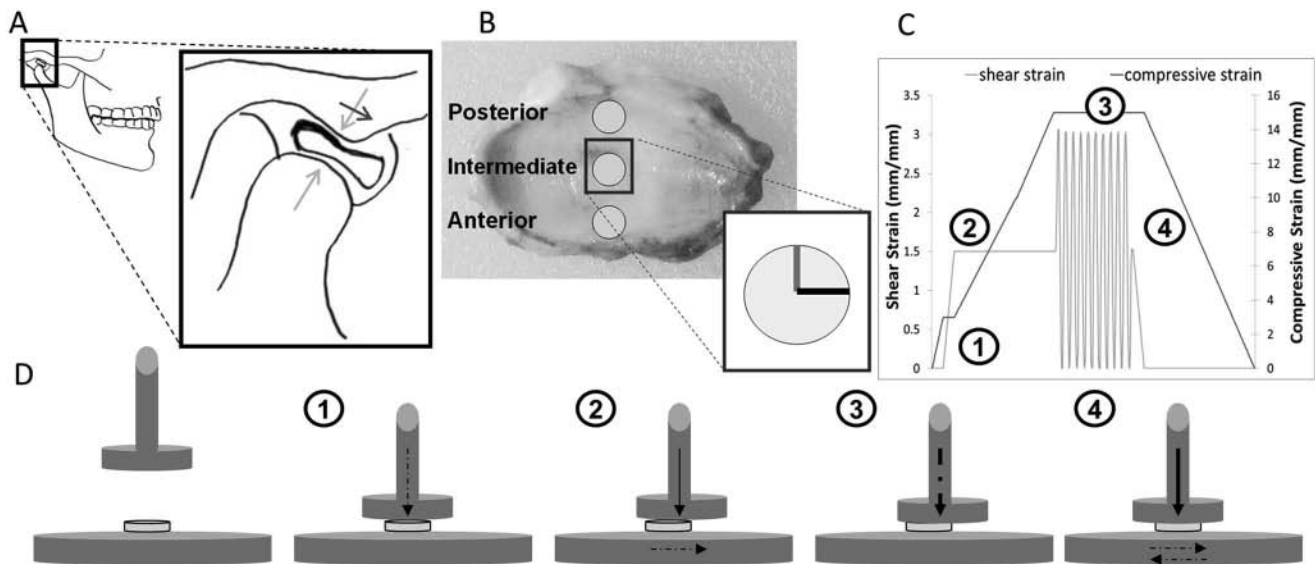
Figure 1. Joint anatomy and simplified free-body diagram, regional sampling, and testing method. **(A)** The gross anatomy of the TMJ and the placement of the disc within the glenoid fossa. The insert illustrates the position of the TMJ disc when the mandibular condyle slides forward with respect to the articular eminence when the jaw opens. **(B)** The sampling regions of the TMJ disc and the directional notation used to orient the sample properly for testing (gray line, anteroposterior direction; black line, mediolateral direction). A representative testing strain profile is shown in **(C)** (description in text body), and **(D)** depicts the sequential testing procedure used to generate the strain profile of (C) (dashed arrows indicate active loading, and solid arrows indicate sustained loading).

3 samples from each disc: anterior, intermediate, and posterior samples (Fig. 1B). Anterior-to-posterior (A-P) and medial-to-lateral (M-L) directions were labeled by means of a water-resistant marker on each disc sample (Fig. 1B, insert), to orient the sample correctly for testing within the hydrated testing chamber.

Sample Groups

The TMJ discs were divided into 3 testing groups—anterior, intermediate, and posterior—each undergoing 27 testing procedures [frequency (F) variation (0.5 Hz, 1 Hz, and 5 Hz), compressive strain (ε) variation (5%, 10%, and 15%), and shear strain (γ) variation (1%, 3%, and 5%)], with 9 specimens for each testing procedure. The order of the testing procedure was randomized for each sample group to minimize sample error (see Appendix 7, Appendix Fig. 3).

Biomechanical Testing – Cyclic Shear Loading

A Biomomentum Mach1 Micromechanical System (Biomomentum Inc., Laval, Quebec, Canada) was used for all mechanical testing. The Mach1 is a multi-axial modular mechanical testing rig which can measure or impart compressive and shear loading. The testing chamber was filled with 0.15 M PBS (pH 7.4) to maintain hydration, similar to the *in vivo* environment (Piette, 1993) and to maintain consistency with previous studies on TMJ tissue mechanics (Tanaka *et al.*, 2003c; Allen and Athanasiou, 2006). An axially translating bottom plate and an axially stationary vertically translating 2.5-cm-diameter indenter were used to generate the shear and compressive loads. Prior to being tested, samples were allowed to equilibrate (unloaded) in PBS for 5 min at 37 ± 1°C.

Sample height was determined by a pre-programmed function of the Mach1 called 'find contact' (see Appendix 2). With the strain profile illustrated in Fig. 1C, compressive and shear strain deformations (indenter displacement, L position; and axially translating bottom plate, x position) were applied to the tissue and assessed according to the calculations $\varepsilon = \Delta L / L_0$ and $\gamma = \Delta x / L_0$, where ΔL is the decrease in sample thickness and Δx is the axial displacement in the shear direction. Both parameters relative to the initial thickness L_0 were needed to produce the desired strain range (see Appendix 6). The Mach1 measures resulting force (F_X and F_Z) experience by the indenter during the compressive and shear loading. The resulting compressive stress on each sample is defined by $\sigma = F_Z/A$, where F_Z is the compressive force and A is the cross-sectional area of the sample, and the resulting shear stress is $\tau = F_x/A$, where F_X is the resulting axial force and A is again the cross-sectional area of the sample (Lumpkins *et al.*, 2008).

Samples were sheared under sinusoidal strain defined by $\gamma = \Delta \gamma \sin(\omega t)$, where $\Delta \gamma$ and ω are the respective strain amplitude and frequency, and t is time. We analyzed results of the cyclic loading tests by calculating the hysteresis, peak stresses, and the instantaneous and steady-state compressive (E_{int}, E_{ss}) and shear moduli (G_{int}, G_{ss}). The general calculations for the compressive and shear moduli are $E = \sigma / \varepsilon$ and $G = \tau / \gamma$, respectively.

Statistical Analysis

Each set of test group data was calculated based on the testing of 9 samples (n = 9). We calculated standard deviations and used one-way analysis of variance (ANOVA) testing to determine statistical significance between and among test groups for biomechanics. Significance was established by the Tukey-Kramer test ($p = 0.05$, n = 9).
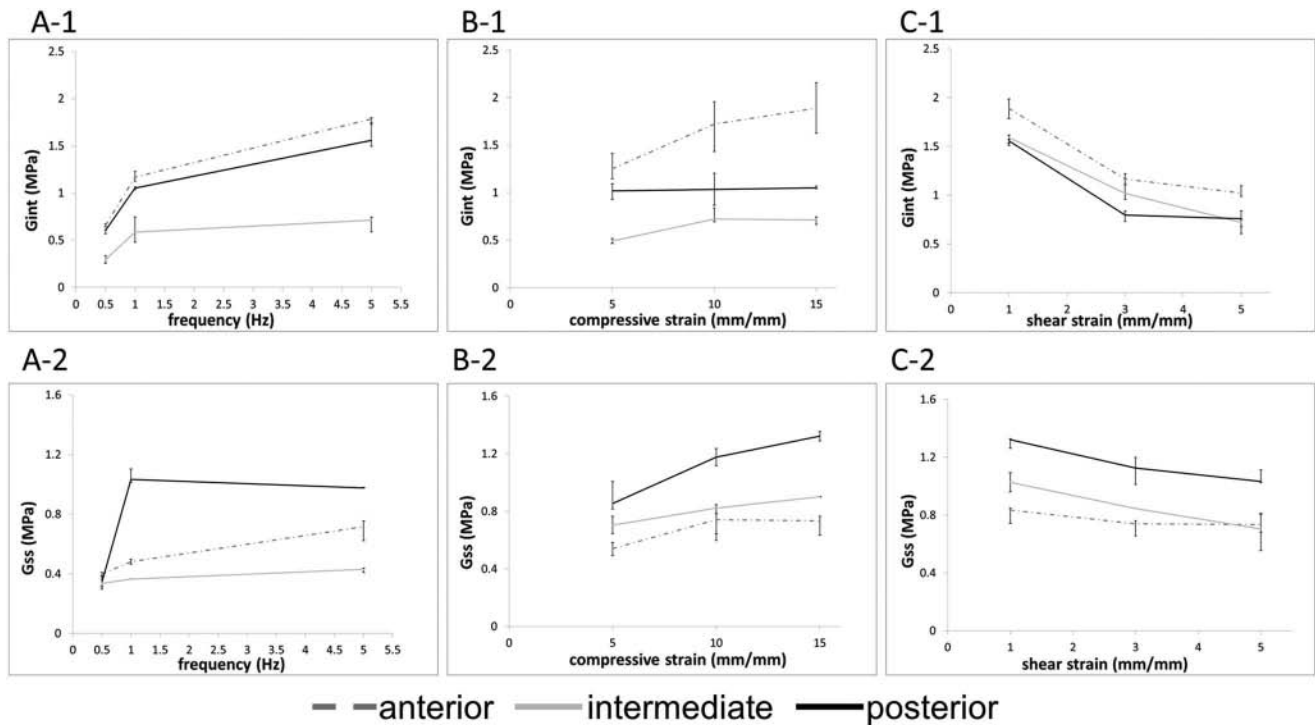
Figure 2. Changes in shear modulus with frequency, compressive strain, and shear strain. Mean values of the instantaneous (1) and steady-state (2) shear moduli as a function of frequency, with $\gamma = 1\%$ and $\varepsilon = 10\%$ **(A),** compressive displacement, F = 1 Hz, and $\gamma = 1\%$ **(B),** or shear displacement, $\varepsilon = 10\%$ and F = 1 Hz **(C).** Samples were shear-strained in the anterior to posterior direction for all data presented. Increases in frequency and compressive strain caused shear stiffening, and the application of greater shear strain induced the shear modulus to become more elastic in the anterior and intermediate regions of the disc. Error bars represent standard deviations.

RESULTS

The average thicknesses reported for the tested regions were 3.66 ± 0.24, 2.00 ± 0.29, and 3.88 ± 1.45 mm for the anterior, intermediate, and posterior regions, respectively. Shear modulus was evaluated for the 1st strain cycle (G_{int}) and for the 10th strain cycle (G_{ss}) to show the changes exerted by frequency and compressive and shear strain on the material properties over the load application (Fig. 2). When shear loads were displaced in the A-P direction, the stiffness of all regions decreased from G_{int} to G_{ss}, with the most noteworthy change occurring with frequency increase (Fig. 2A). Change in G_{int}, evaluated solely as a function of frequency increase from 0.5 Hz to 5 Hz, was, on average, an 8.6% increase for all ε and γ conditions evaluated. When compressive strain was increased and the other test conditions were maintained, the disc experienced a similar increase in shear modulus (Fig. 2B); however, when the shear strain was increased, the shear modulus decreased, becoming more elastic (Fig. 2C). Most noticeably, for the posterior region tested at the high frequency (5 Hz) and high compressive strain (15%) (data not represented in Fig. 2C), $G_{int} = 1.556 \pm 0.327$ MPa and $G_{ss} = 0.797 \pm 0.315$ MPa at $\gamma = 1\%$ and $G_{int} = 1.078 \pm 0.158$ MPa and $G_{ss} = 0.686 \pm 0.072$ MPa at $\gamma = 5\%$, an average decrease of 22.5% from the instantaneous to the steady-state condition.

Similar to the shear modulus change with γ (Fig. 2C), the compressive modulus also became more elastic with repeated shear in all regions of the disc (Fig. 3). The cycle-dependent compressive modulus of the posterior region shows that, with each shear cycle application, the compressive modulus increased by nearly 5% of the E_{int} value before continuing the decreasing trend. The average magnitude of the ΔE (peak height) when sheared in the A-P direction was 1.5 ± 0.0 kPa, and in the M-L direction was 0.40 ± 0.03 kPa in the posterior region, and became more regular as the compressive modulus reached a steady-state condition (cycles 6 through 10). This phenomenon was also seen in the anterior region, but only when shear strain was applied in the M-L direction, and the magnitude was less than 25% of the posterior regions ΔE (table in Fig. 3).

The shear modulus characteristics are described in Fig. 4. Only the posterior region statistically maintained its shear modulus from G_{int} to G_{ss} when sheared in the A-P direction. All regions when sheared in the M-L direction maintained within 20% of their G_{int} stiffness over the strain application cycle.

DISCUSSION

The ability of the TMJ disc to act as a buffer between the articulating skeletal structures of the TMJ is fundamental to jaw movement; thus, it is paramount to understand the mechanical response of a healthy TMJ disc when exposed to loading similar to that experienced *in vivo*. The current investigation focused on the mechanical characteristics of the disc during cyclic shear
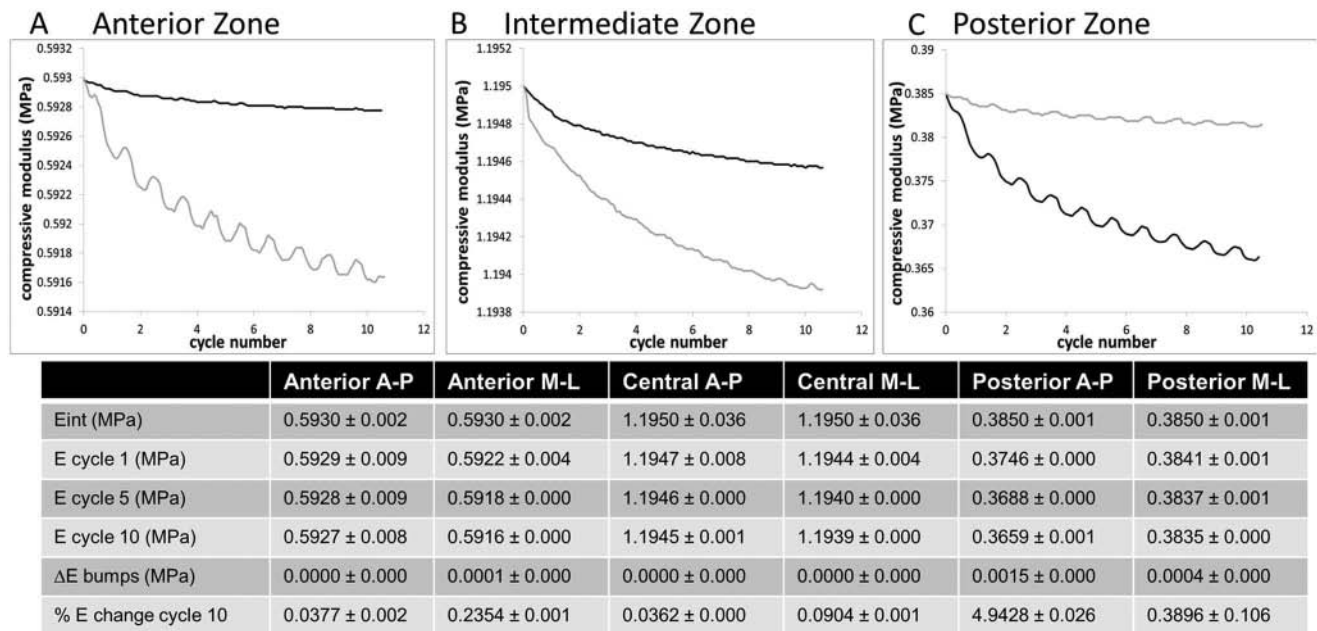
Figure 3. Changes in compressive modulus when cyclic shear strain was applied in the anterior-to-posterior or medial-to-lateral direction. Representative zonal compressive modulus evolutions over the load application are shown in **(A)**, **(B)**, and **(C).** Mean values of the compressive modulus of each region of the TMJ disc are shown in the table. The anterior and intermediate regions had less reduction of their compressive modulus, retaining their compressive modulus even when repeatedly sheared. The posterior region became more elastic with application of shear strain. All regions had significant reduction in initial to steady-state modulus when sheared in the medial-lateral direction ($p < 0.05$). Anterior-posterior shear strain application data are represented by the black curves, and medial-lateral shear strain application data are represented by the gray curves.
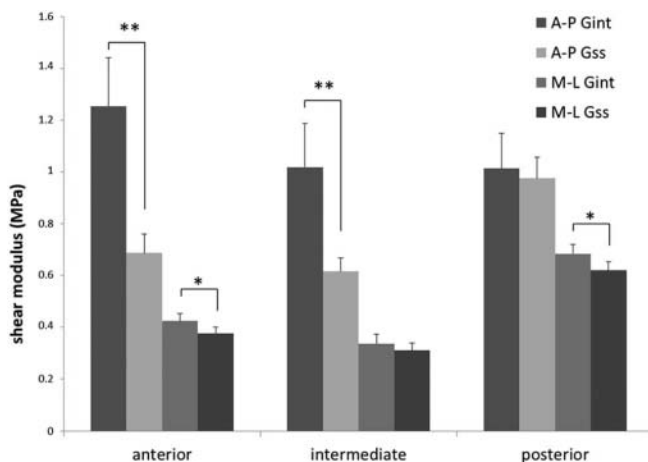

Figure 4. Mean regional values of the instantaneous and steady-state shear moduli of each disc region when strained in the anterior-to-posterior direction and the medial-to-lateral direction. The anterior and central regions experienced a significant decrease in shear modulus when strained in the anterior-posterior (A-P) direction. This increased elasticity was not seen in the posterior region (*$p < 0.05$; **$p < 0.01$).

testing, when the magnitude of shear strain (γ), compressive strain (ε), and frequency (F) are varied under broadly physiological parameters (see Appendix 5).

Previous investigations by Tanaka and co-workers have shown that the disc experiences shear stiffening, or increase in elastic modulus, as ε or F is increased, and, conversely, shear softening with increasing γ (Tanaka *et al.*, 2003b, 2004). Fig. 2 depicts the dependency of the disc regions on frequency, compressive strain, and shear strain. Shear stiffening was hypothesized to be a combination of 2 effects: the first due to interstitial fluid or bulk matrix outflow as pressurized fluids are squeezed from the point of strain application; and the second due to the frequency of γ application being increased, which results in a lag in fluid resorption between the successive strain applications. These conclusions were further supported by our results and can be expanded to be a universal trend for the regions tested. The shear softening with increased shear strain, however, was observed only in the anterior and intermediate regions of the disc. It has previously been hypothesized that observed shear softening is due to the proteoglycan [glycosaminoglycan (GAG)] component and water matrix within the disc possessing non-Newtonian characteristics. GAGs are highly hydrophilic sugar chains that act to maintain the disc's resistance to pressure. The lack of significant shear softening in the posterior region, then, is in agreement with this hypothesis, since the posterior band of the disc contains a lower GAG content than the anterior or intermediate zones (Nakano and Scott, 1996; Almarza *et al.*, 2006) (Fig. 4). A difference between our experimental design and that of Tanaka *et al.* is that the latter's work evaluated the shear properties of the porcine disc at porcine core temperature (39°C), and our evaluation was done at human body temperature. This temperature difference may account for the

variances in our mechanical results, since higher temperatures reduce stiffness and strength of the disc, since many ECM components (collagen and proteoglycans) are temperature-sensitive (Detamore and Athanasiou, 2003).

Application of cyclic shear in the A-P direction decreased the compressive modulus until a steady state was reached; however, in the posterior region, significant 'bumps' were observed in the mechanical profile (Fig. 3C). We hypothesized that the increase in compressive stiffness associated with these bumps represents a material property that acts as a breaking system (force). Compression causes outflow of interstitial fluid or a shifting of the bulk matrix from the point of strain application. As the fluid matrix shifts, the periphery swells to maintain the tissue volume and causes increased hoop stresses and hydraulic pressures that inhibit the force dispersion and act to recoil the fibers back toward their undistorted orientation. Compressive properties of the disc are strongly dependent on interstitial fluid flow (Allen and Athanasiou, 2006), and with fewer paths for tissue fluid to escape when the disc is under shear, E will respond in intermittent increased stiffness. A possible limitation of these investigations is that we evaluated disc punches that did not necessarily retain the boundary conditions of the whole disc; however, the ECM fiber alignment superstructure remained intact. This trend was observed only in the anterior and posterior zones, likely due to fiber arrangement, where collagen fibers were oriented in a mediolateral arc that increased hoop stresses and hydrostatic forces (Detamore *et al.*, 2005; Almarza and Athanasiou, 2006). By comparison, the intermediate region, where the collagen fibers were aligned in the antero-posterior direction, was shown to culminate in channels that shuttled interstitial fluid quickly within the region. The mechanical consequence is that the intermediate zone was more elastic than the periphery of the disc (Lumpkins and McFetridge, 2009).

Perforation is often associated with disc derangement or osteoarthritis; however, tearing of the posterior-lateral region is also seen in asymptomatic discs (Kuribayashi *et al.*, 2008; Liu *et al.*, 2010). The results of the current study showed that the steady-state shear modulus was stiffest in the disc's posterior region, indicating that this region is different structurally and/or in composition. These mechanical results are in agreement with clinical observations of regional disc damage. It is clinically accepted that TMJ disc fatigue occurs most frequently in the disc's lateral-posterior region (Kuribayashi *et al.*, 2008). We hypothesized that this retained stiffness with repeated shear strain applications limits the disc's ability to distribute (disseminate) loads away from the impact point, leading to greater residual localized stress summation. It was further hypothesized that these localized stresses result in material fatigue and eventual failure, seen clinically as disc perforations.

Shear strain in the M-L direction is less prominent in healthy TMJ disc loading (Fushima *et al.*, 1995; Athanasiou *et al.*, 2009). However, shear strain is associated with the non-pathological tooth-grinding and jaw-clenching that are seen in bruxism, which can potentially lead to TMDs (Kuboki *et al.*, 1996; Nagahara *et al.*, 1999; Gallo *et al.*, 2000). Sometimes simplified as hyperactivity of the *lateral* pterygoid, clenching and bruxing mechanics are more completely described as parafunctional activity of 1 or more of the major masticatory muscles

(masseter, medial pterygoid, temporalis, and lateral pterygoid) (Nagahara *et al.*, 1999; Hirose *et al.*, 2006). The mechanical testing of the disc's elastic moduli when sheared in the M-L direction under high compressive load is meaningful for the assessment of any potential relationship between bruxing and TMJ disc perforation. Similar to the shear modulus characteristics of the posterior region under A-P shear, all regions of the disc have an observable trend of retaining their shear modulus from G_{int} to G_{ss} when load is applied with M-L loading (Fig. 4).

In conclusion, these results confirm that the mechanical characteristics of the TMJ disc are highly dependent on the ECM microenvironment and its regional composition. The posterior region of the disc, which is the most commonly observed zone in which the disc shows fatigue, has been shown to maintain its stiffness when compressed or sheared cyclically. While there is no direct association between theoretical or experimental models and the clinical experience, these results are in agreement with mathematical modeling results showing that large stresses developed in the posterior region of the disc and retrodiscal tissue during prolonged clenching, and higher still in these regions when antero-lateral internal derangement is included (Hirose *et al.*, 2006; Nishio *et al.*, 2009). The hypothesis that there is a relationship between the disc's regional mechanical properties and common clinical observations of TMJ disc damage is supported by the data collected in these works. These results support further investigation of fluid movement within the disc scaffold and greater development of a physiologically representative testing regime.

ACKNOWLEDGMENTS

REFERENCES

Allen K, Athanasiou K (2005). A surface-regional and freeze-thaw characterization of the porcine temporomandibular joint disc. *Ann Biomed Eng* 33:951-962.

Allen K, Athanasiou K (2006). Viscoelastic characterization of the porcine temporomandibular joint disc under unconfined compression. *J Biomech* 39:312-322.

Almarza A, Athanasiou K (2006). Effects of hydrostatic pressure on TMJ disc cells. *Tissue Eng* 12:1285-1294.

Almarza A, Bean A, Baggett L, Athanasiou K (2006). Biochemical analysis of the porcine temporomandibular joint disc. *Br J Oral Maxillofac Surg* 44:124-128.

Athanasiou KA, Almarza AA, Detamore MS, Kalpakci KN (2009). Tissue engineering of temporomandibular joint cartilage. San Rafael, CA: Morgan & Claypool Publishers.

Callaghan J, McGill S (2001). Intervertebral disc herniation: studies on a porcine model exposed to highly repetitive flexion/extension motion with compressive force. *Clin Biomech (Bristol, Avon)* 16:28-37.

Detamore M, Athanasiou K (2003). Tensile properties of the porcine temporomandibular joint disc. *J Biomech Eng* 125:558-565.

Detamore M, Orfanos J, Almarza A, French M, Wong M, Athanasiou K (2005). Quantitative analysis and comparative regional investigation of

the extracellular matrix of the porcine temporomandibular joint disc. *Matrix Biol* 24:45-57.

Fushima K, Gallo L, Krebs M, Palla S (1995). Medial and lateral TMJ space variations during mastication. *J Dent Res* 74(Spec Iss):588, abstract #1504.

Gallo L, Nickel J, Iwasaki L, Palla S (2000). Stress-field translation in the healthy human temporomandibular joint. *J Dent Res* 79:1740-1746.

Hirose M, Tanaka E, Tanaka M, Fujita R, Kuroda Y, Yamano E, *et al*. (2006). Three-dimensional finite-element model of the human temporomandibular joint disc during prolonged clenching. *Eur J Oral Sci* 114:441-448.

Iatridis J, ap Gwynn I (2004). Mechanisms for mechanical damage in the intervertebral disc annulus fibrosus. *J Biomech* 37:1165-1175.

Koolstra JH, Tanaka E, Van Eijden TM (2007). Viscoelastic material model for the temporomandibular joint disc derived from dynamic shear tests or strain-relaxation tests. *J Biomech* 40:2330-2334.

Kuboki T, Azuma Y, Orsini M, Takenami Y, Yamashita A (1996). Effects of sustained unilateral molar clenching on the temporomandibular joint space. *Oral Surg Oral Med Oral Pathol Oral Radiol Endod* 82:616-624.

Kuo J, Zhang L, Bacro T, Yao H (2010). The region-dependent biphasic viscoelastic properties of human temporomandibular joint discs under confined compression. *J Biomech* 43:1316-1321.

Kuribayashi A, Okochi K, Kobayashi K, Kurabayashi T (2008). MRI findings of temporomandibular joints with disk perforation. *Oral Surg Oral Med Oral Pathol Oral Radiol Endod* 106:419-425.

Lai W, Bowley J, Burch J (1998). Evaluation of shear stress of the human temporomandibular joint disc. *J Orofac Pain* 12:153-159.

Liu XM, Zhang SY, Yang C, Chen MJ, Y Cai X, Haddad MS, *et al*. (2010). Correlation between disc displacements and locations of disc perforation in the temporomandibular joint. *Dentomaxillofac Radiol* 39:149-156.

Lumpkins S, McFetridge P (2009). Regional variations in the viscoelastic compressive properties of the temporomandibular joint disc and implications toward tissue engineering. *J Biomed Mater Res A* 90:784-791.

Lumpkins S, Pierre N, McFetridge P (2008). A mechanical evaluation of three decellularization methods in the design of a xenogeneic scaffold for tissue engineering the temporomandibular joint disc. *Acta Biomater* 4:808-816.

Nagahara K, Murata S, Nakamura S, Tsuchiya T (1999). Displacement and stress distribution in the temporomandibular joint during clenching. *Angle Orthod* 69:372-379.

Nakano T, Scott P (1996). Changes in the chemical composition of the bovine temporomandibular joint disc with age. *Arch Oral Biol* 41:845-853.

Nishio C, Tanimoto K, Hirose M, Horiuchi S, Kuroda S, Tanne K, *et al*. (2009). Stress analysis in the mandibular condyle during prolonged clenching: a theoretical approach with the finite element method. *Proc Inst Mech Eng H* 223:739-748.

Piette E (1993). Anatomy of the human temporomandibular joint. An updated comprehensive review. *Acta Stomatol Belg* 90:103-127.

Tanaka E, del Pozo R, Tanaka M, Aoyama J, Hanaoka K, Nakajima A, *et al*. (2003a). Strain-rate effect on the biomechanical response of bovine temporomandibular joint disk under compression. *J Biomed Mater Res A* 67:761-765.

Tanaka E, Hanaoka K, van Eijden T, Tanaka M, Watanabe M, Nishi M, *et al*. (2003b). Dynamic shear properties of the temporomandibular joint disc. *J Dent Res* 82:228-231.

Tanaka E, Kawai N, van Eijden T, Watanabe M, Hanaoka K, Nishi M, *et al*. (2003c). Impulsive compression influences the viscous behavior of porcine temporomandibular joint disc. *Eur J Oral Sci* 111:353-358.

Tanaka E, Kikuzaki M, Hanaoka K, Tanaka M, Sasaki A, Kawai N, *et al*. (2003d). Dynamic compressive properties of porcine temporomandibular joint disc. *EurJ Oral Sci* 111:434-439.

Tanaka E, Kawai N, Hanaoka K, van Eijden T, Sasaki A, Aoyama J, *et al*. (2004). Shear properties of the temporomandibular joint disc in relation to compressive and shear strain. *J Dent Res* 83:476-479.